

Published in final edited form as:

*Contrast Media Mol Imaging*. 2009 July ; 4(4): 165–173. doi:10.1002/cmml.276.

## The influence of ferucarbotran on the chondrogenesis of human mesenchymal stem cells

Tobias D Henning, MD<sup>1,2</sup>, Elizabeth J Sutton, MD<sup>1,3</sup>, Anne Kim<sup>4</sup>, Daniel Golovko, MD<sup>1</sup>, Andrew Horvai, MD<sup>5</sup>, Larry Ackerman<sup>6</sup>, Barbara Sennino, PhD<sup>6</sup>, Donald McDonald, MD, PhD<sup>6</sup>, Jeffrey Lotz, PhD<sup>4</sup>, and Heike E Daldrop-Link, MD, PhD<sup>1</sup>

<sup>1</sup> Department of Radiology, UCSF Medical Center, University of California, San Francisco, CA, USA

<sup>2</sup> Department of Radiology, Technical University of Munich, Munich, Germany

<sup>3</sup> Department of Medicine, Boston University, Boston, MA, USA

<sup>4</sup> Department of Orthopedic Surgery, University of California, San Francisco, CA, USA

<sup>5</sup> Department of Pathology, UCSF Cancer Center, University of California, San Francisco, CA, USA

<sup>6</sup> Department of Anatomy, University of California, San Francisco, CA, USA

### Abstract

For in vivo applications of magnetically labeled stem cells, biological effects of the labeling procedure have to be precluded. This study evaluates the effect of different Ferucarbotran cell labeling protocols on chondrogenic differentiation of human mesenchymal stem cells (hMSC) as well as their implications for MR imaging.

hMSC were labeled with Ferucarbotran using various protocols: Cells were labeled with 100µg Fe/ml for 4h and 18h and additional samples were cultured for 6 or 12 days after the 18-hour labeling. Supplementary samples were labeled by transfection with protamine sulfate. Iron uptake was quantified by ICP-spectrometry and labeled cells were investigated by transmission electron microscopy and by immunostaining for ferucarbotran. The differentiation potential of labeled cells was compared to unlabeled controls by staining with alcian blue and hematoxylin & eosin, then quantified by measurements of glucosaminoglycans (GAG). Contrast agent effect at 3T was investigated on day 1 and day 14 of chondrogenic differentiation by measuring signal-to-noise ratios on T2-SE and T2\*-GE-sequences.

Iron uptake was significant for all labeling protocols ( $p < 0.05$ ). The uptake was highest after transfection with protamine sulfate ( $25.65 \pm 3.96$  pg/cell) and lowest at an incubation time of 4h without transfection ( $3.21 \pm 0.21$  pg/cell). While chondrogenic differentiation was decreased using all labeling protocols, the decrease in GAG synthesis was not significant after labeling for 4h without transfection. After labeling by simple incubation, chondrogenesis was found to be dose-dependent. MR imaging showed markedly lower SNR values of all labeled cells compared to the unlabeled controls. This contrast agent effect persisted for 14 days and the duration of differentiation.

Magnetic labeling of hMSC with ferucarbotran inhibits chondrogenesis in a dose-dependent manner when using simple incubation techniques. When decreasing the incubation time to 4h, inhibition of chondrogenesis was not significant.

## Keywords

MR Imaging; Molecular Imaging; Stem cells; Cartilage; Tissue Engineering; Iron Oxides; Cell Tracking

---

## Introduction

Matrix-associated stem cell implantation (MASI) therapies have been developed to provide regeneration of bone and cartilage defects of arthritic joints. Human mesenchymal stem cells (hMSCs) are a promising and realistic tool for cell-based therapies, because they are easily obtained by a bone marrow aspirate, well characterized and efficiently expanded in vitro.

The plasticity and capacity for self-renewal generate the unique potential of hMSCs for synovial joint regeneration. hMSCs can differentiate into all components of a synovial joint, such as bone, cartilage, tendons, fat, and muscle [1,2]. In recent years, various techniques and protocols for hMSC differentiation into bone and cartilage have been developed. Such techniques include dedicated growth factors [3] or culture substrates [4] to trigger directed differentiation in 3D matrixes [5–7].

hMSCs can be labeled with iron oxide nanoparticles and can be visualized non-invasively in vivo with MR imaging over several days [8,9]. Direct non-invasive in vivo visualization of hMSC transplants in cartilagenous defects would improve spatio-temporal monitoring and allow a non-invasive confirmation of stem cell homing and engraftment or an early diagnosis of graft failure due to cell death or migration from the transplantation site.

The potential clinical application of this imaging technique require that labels, such as iron oxide, do not impair the viability or function of the transplanted stem cells. Recently, Bulte et al. reported impaired chondrogenesis of hMSCs after labeling with 50µg Fe/ml Ferumoxides-polylysine for 24 hours [10]. This may have been dose-dependent, since the same authors demonstrated a smaller degree of impairment after incubation with half of the initial contrast agent concentration [11]. Finally, the same authors showed that Protamine sulfate by itself does not inhibit chondrogenic differentiation [11].

An alternative iron oxide contrast agent is Ferucarbotran (Resovist), which is approved for clinical applications in Europe. In comparison to Ferumoxides, it has a higher labeling efficiency for non-phagocytic cells [12] and a higher threshold for toxic effects than Ferumoxides [13] i.e. impaired viability and/or apoptosis of labeled cells was noted at higher iron concentrations of Ferucarbotran when compared to ferumoxides. It has also been shown that hMSC can be efficiently labeled with Ferucarbotran without the need of a transfection agent [14,15].

Thus, the purpose of this study was to evaluate the effect of Ferucarbotran labeling on the differentiation potential of hMSCs into chondrocytes. We compared the effect of different iron concentrations and labeling techniques on hMSC differentiation in order to determine the optimal protocol that would provide the least impairment of the differentiation process.

## Experimental

### Contrast Agent

The MR contrast agent Ferucarbotran (Resovist, Schering AG, Berlin, Germany) was used for this study. Ferucarbotran is a superparamagnetic iron oxide (SPIO) particle with a crystalline nonstoichiometric Fe<sup>2+</sup> and Fe<sup>3+</sup> iron oxide core. A carboxydextran coat with a mean

hydrodynamic diameter of 62 nm stabilizes the particle, ensures aqueous solubility and results in a net negative charge for the particle [16–18]. The  $r_1$  and  $r_2$  relaxivities are  $7.2 \pm 0.1 \text{ mM}^{-1}\text{s}^{-1}$  and  $82.0 \pm 6.2 \text{ mM}^{-1}\text{s}^{-1}$  respectively (in blood at  $37^\circ\text{C}$  and 1.5 T) [18]. Ferucarbotran was approved for clinical MR imaging of the liver in Europe in 2001 [17]. Ferucarbotran can also be used for ex vivo cell labeling and subsequent in vivo tracking of labeled cells. The iron oxide particles are internalized into cells by endocytosis and then stored in secondary lysosomes within the cytoplasm [13].

### Cell Culture and Cell labeling

Human mesenchymal stem cells (hMSC, Lonza Walkersville, Inc., Walkersville, MD, USA), were cultured in Dulbecco's Modified Eagle Medium (DMEM) High Glucose media (Invitrogen, Carlsbad, CA) supplemented with 10% fetal bovine serum (FBS, Hyclone, Logan, UT, USA) and 1% Penicillin-Streptomycin in a humidified 5%  $\text{CO}_2$  atmosphere at  $37^\circ\text{C}$ . Cells were passaged upon 90% confluency and either used for experiments or redistributed to new culture flasks. All experiments were performed in between passages 6–10 to avoid senescence and ensure full chondrogenic potential.

The cells were labeled with Ferucarbotran (Resovist<sup>®</sup>, stock concentration: 500 mmol Fe/ml, Bayer Schering AG, Berlin, Germany) using the following incubation protocols:

- (1a) Standard protocol [15]:  $1.5 \times 10^6$  hMSC were incubated for 18 hours with Ferucarbotran at a concentration of  $100 \mu\text{g Fe/ml}$  in 20 ml of serum free media in  $175 \text{ cm}^2$  tissue culture flasks (Nalge Nunc, Rochester, NY, USA).
- (1b) Standard protocol + continuous culture of the labeled hMSC for 6 days
- (1c) Standard protocol + continuous culture of the labeled hMSC for 12 days

The rationale behind the variation in protocol was based upon our histopathologic observation that some SPIO remains attached to the cell surface directly after the labeling process and are not completely removed by repetitive washing procedures. Since hMSCs need cell-cell contact for chondrogenic differentiation our hypothesis was that culturing of the labeled cells before induction of chondrogenesis might decrease the amount of membrane-bound SPIO thereby improving chondrogenic differentiation.

- (2) Incubation of hMSC with Ferucarbotran at a concentration of  $100 \mu\text{g Fe/ml}$  for 4h. The rationale behind this protocol was the hypothesis that a decreased intracellular SPIO concentration might improve chondrogenic differentiation.
- (3) Incubation of hMSC with Ferucarbotran at a concentration of  $50 \mu\text{g Fe/ml}$  and Protamine Sulfate ( $5 \mu\text{g/ml}$ , American Pharmaceutical Partners, Schaumburg, IL) for 4h. This protocol was chosen as a corresponding technique to the previously described techniques for cell labeling with the different contrast agent ferumoxides [19,20].

Cells were labeled in T  $175 \text{ cm}^2$  tissue culture flasks (Nalge Nunc, Rochester, NY, USA) with 20 ml of labeling media. All labeling solutions were prepared with serum-free media. For all protocols using simple incubation, FBS was added to a final concentration of 10% after 2h of initial incubation with labeling media. For protocol (3) using protamine sulfate an equal amount of media containing 20% FBS was added after 2 hours of incubation. FBS was added in order to maintain the standardized culture environment and thereby to prevent undirected differentiation. After the cell labeling procedures, the cells were trypsinized and washed three times with PBS (pH 7.4) by sedimentation ( $25^\circ\text{C}$ , 400 g, 5min) and resuspended in complete DMEM growth media. Cellular viability of labeled cells and unlabeled controls was assessed by the trypan blue exclusion assay (Sigma Aldrich, St. Louis, MO). The concentration of iron within the labeled hMSCs was determined by inductively coupled plasma atomic emission spectrometry (ICP-AES, IRIS Advantage, Thermo Jarrell-Ash, MA, USA). For this, triplicate

samples of  $5 \times 10^5$  unlabeled and labeled cells were collected in 400 $\mu$ l of media containing no supplements. Intracellular iron uptake is known to be inhomogenous for different cell types and different labeling protocols [21,22] and therefore results are presented as mean intracellular iron content.

### Chondrogenic differentiation

Chondrogenic differentiation of triplicate samples of Ferucarbotran labeled hMSCs (as explained above) and of unlabeled controls was induced following a standardized protocol [19,23] (Lonza, Walkersville, MD, USA). In brief, aliquots of  $2.5 \times 10^5$  hMSCs were resuspended in 0.5ml of complete chondrogenic media (Lonza) containing 10ng/ml rTGF- $\beta$ 3 (both Lonza). The cell suspension was transferred into polypropylene centrifuge tubes (VWR, West Chester, PA, USA) and centrifuged at 150 g for 5 minutes. Pellets were then incubated at 37°C and 5% CO<sub>2</sub> for 14 days. The media was changed every 2 days and chondrogenic pellets were harvested after 14 days in culture.

### GAG quantification

Quantification for accumulated sulfated glycosaminoglycan (s-GAG) was performed as previously described [24,25]. In brief, each pellet was digested at 65°C overnight with 1 ml of papain solution (25g/mL in 50 mM of sodium phosphate, 2 mM of N-acetyl cysteine, 2 mM of EDTA, pH 6.5). The dimethylmethylene blue (DMMB) assay was used to determine the s-GAG content of papain digests, using chondroitin sulfate C (sodium salt from shark cartilage, Sigma, St. Louis, Missouri) as a standard. A microplate reader was used for spectrophotometric measurements (Model 3550, BioRad; Hercules, California, USA).

### Magnetic Resonance Imaging

The chondrogenic pellets underwent MR imaging at 3T on days 1 and 14 of chondrogenic differentiation on a clinical MR scanner (Signa EXCITE HD 3T, GE Medical Systems, Milwaukee, WI, USA) using a standard circularly polarized quadrature knee coil (Clinical MR Solutions, Brookfield, WI, USA). The tubes containing the pellets were immersed in a water bath to avoid susceptibility artifacts from surrounding air and then scanned at room temperature (20°C). MR images were obtained using axial and coronal spin echo (SE) sequences with a fixed TR of 2000 ms and multiple TE (60, 45, 30, 15 ms) values. In addition, T<sub>2</sub>\*-weighted axial and coronal gradient echo (GE) images were obtained with a flip angle of 30 degree, a fixed TR of 500 ms and varying TE values (28.8, 14.4, 7.2, 3.7 ms). All sequences were acquired with a field of view (FOV) of 160x160 mm, a matrix of 256x196 pixels, a slice thickness of 5 mm and one acquisition.

### MR Data analysis

MR images were transferred as DICOM images to a SUN/SPARC workstation (Sun Microsystems, Mountain View, CA, USA) and analyzed using a dicom-dedicated image processing software (Osirix, UCLA, Los Angeles, CA). Signal intensities (SI) of the different pellets and SI of background noise were measured on coronal MR images, using operator-defined regions of interest (ROI). Average size of ROIs measured 6mm<sup>2</sup>. For measurements of background noise, ROIs were placed in the air surrounding the waterbath. The MR signal of each pellet was quantified as signal-to-noise-ratio (SNR):  $SNR = SI_{(pellet/noise)}$  [26]. Care was taken to analyze only data points with signal intensities significantly above the noise level. SNR was compared in between labeled cell pellets and unlabeled controls.

### Electron Microscopy

Control and labeled cells were plated on Thermanox coverslips and let adhere as adherent cell cultures overnight. They were then fixed directly on the slides with 2% glutaraldehyde in 0.1M

sodium cacodylate buffer, postfixed with 1% osmium tetroxide followed by 2% aqueous uranyl acetate. The samples were dehydrated with ethanol and embedded in epoxy resin. Ultrathin sections of 80 nm were stained with 2% uranyl acetate and Reynolds lead-citrate. They were examined and photographed at 80kV in a JEOL 100CX II (JEOL, Tokyo, Japan).

### Confocal Microscopy

Control and labeled cells were plated on multichamber glass slides (Nunc, Rochester, NY, USA) and cultured as described above. Once attached, cells were fixed at room temperature with Carnoy's solution and washed three times with PBS. Samples were then incubated with an anti-dextran FITC antibody (Stem Cell Technologies, Tukwila, WA, USA) at room temperature for 60 minutes to stain for dextran-coated iron oxides. Finally, slides were washed three times with PBS and counterstained with DAPI (Vectashield with DAPI, Vector Laboratories, Burlingame, CA, USA). Samples were analyzed by confocal microscopy at 40x (Zeiss LSM 510, Thornwood, NY, USA).

### Histopathology of labeled cells and chondrogenic pellets

Chondrogenic pellets were stained with hematoxylin & eosin (H&E) for structural analysis. They were also stained with alcian blue for glucosaminoglycans to evaluate cartilage matrix deposition. The pellets were washed in PBS, fixed in 10% Neutral Buffered Formalin and encapsulated in HistoGel (both Richard-Allan Scientific, Kalamazoo, MI, USA). After paraffin embedding, sections of 5µm thickness were cut and stained with H&E and alcian blue. H&E sections were evaluated for the presence, distribution and morphology of cells. Each section was scored to assess the fraction of spindle cells as follows: 0 = 0 %, 1 = 1 – 33 %, 2 = 34 – 66 %, 3 = 67 – 100%. The intensity of alcian blue staining was used to quantitate the abundance of cartilage matrix, as follows: + = weak stain, ++ = moderate stain, +++ = most intense stain.

### Statistical analysis

Statistical calculations were performed using the statistical software SPSS (SPSS Inc. Chicago, Illinois, USA). Measurements of cell viability, of cellular iron uptake and of GAG content in cell pellets were acquired in triplicates. Mean values and standard deviations were calculated. Labeled samples were compared with unlabeled controls for significant differences with a t-test on a 5%-level of significance. Repeated pairwise comparisons of one sample were adjusted with the Bonferroni correction.

## Results

### Cell labeling and spectrometry

Trypan blue staining showed no significant decrease of cell viability of labeled cells (Table 1). Spectrometry measurements showed that all incubation protocols resulted in a significant mean cellular uptake of iron oxides compared to unlabeled controls (Figure 1, Table 1). The uptake of Ferucarbotran into hMSCs was significantly higher after simple incubation with Ferucarbotran for 18 h compared to 4h ( $p = 0.0002$ ). Cellular uptake of Ferucarbotran was significantly increased after transfection with protamine sulfate, regardless of incubation time ( $p < 0.05$ ). The iron content of the hMSCs labeled with the standard protocol was not significantly decreased at 6 days after labeling, but was significantly decreased at 12 days after labeling ( $p = 0.15$  vs  $p = 0.0001$ ). The iron uptake could be macroscopically appreciated as brown staining of the chondrogenic cell pellets (Figure 1).

### GAG production of chondrogenic pellets

All Ferucarbotran labeled chondrogenic cell pellets showed reduced GAG synthesis compared to unlabeled controls. This difference was significant for all labeled pellets except for the



100 $\mu$ g 4h sample. All chondrogenic cell samples showed an inverse relation between GAG production and iron uptake, except for the sample labeled with ferucarbotran and protamine sulfate (Figure 1). hMSCs labeled with Ferucarbotran for only 4 hours showed a significantly higher GAG production compared to hMSCs that had been labeled with Ferucarbotran for 18 h. In addition, hMSCs that had been cultured for 6 or 12 days in between labeling and induction of chondrogenesis showed a higher level of GAG synthesis compared to labeled hMSCs, which had undergone chondrogenic differentiation directly after 18 h labeling.

### MR imaging of chondrogenic cell pellets

MR images of chondrogenic pellets showed a very similar contrast agent effect on day 1 and on day 14 of chondrogenic differentiation. There was marked signal loss of labeled hMSCs compared to the unlabeled controls on T2 and T2\* images (Figure 2). This area of signal loss exceeded the size of the labeled cell pellets. Corresponding SNR values were at least 10-fold lower for all labeled cell pellets compared to the unlabeled controls (Figure 2). SNR data of labeled pellets (representing the magnitude of signal loss) were not different for the applied T2 and T2\* sequences. However, the susceptibility effects of labeled pellets (i.e. area of signal loss) were larger on T2\* compared to T2-images. It was not possible to evaluate either T2 or T2\* relaxation times for chondrogenic cell pellets because the MRI signal of the cell pellets was at the noise level using the minimal TE setting of our clinical scanner. Therefore, we compared the signal-to-noise ratios based on T2 and T\*2 sequences.

### Confocal microscopy and electron microscopy of labeled hMSCs

Confocal microscopy studies of labeled hMSCs, stained with anti-dextran FITC antibody showed contrast agent associated with the cells (Figure 3). It was found that fluorescent staining varied in intensity in between cells labeled with the same protocol. By comparison, the unlabeled control cells did not show any fluorescence. Electron microscopy studies confirmed the presence of iron oxide nanoparticles in secondary lysosomes of labeled cells, but not in unlabeled cells. Electron microscopy also showed clusters of iron oxide particles next to the cell surface for our standard protocol but no extracellular iron for all other protocols. hMSCs labeled by simple incubation for 18 h showed a higher number of iron oxide particle-containing lysosomes compared to hMSCs labeled for 4h. Similarly, hMSCs directly after 18h Ferucarbotran labeling showed more iron oxide-containing lysosomes than hMSCs, which had been cultured for 6 or 12 days after labeling. hMSCs labeled with the transfection agent Protamine sulfate showed fewer but larger iron oxide-filled lysosomes compared to hMSCs that had been labeled without transfection agent. The intensity of FITC staining on confocal microscopy and the amount of intracellular iron on electron microscopy images correlated well with the iron uptake measurements as acquired by spectrometry.

### Histology of chondrogenic pellets

After chondrogenic differentiation for 14 days, the pellets showed different degrees of chondrogenesis. Representative samples are shown in Figure 3 and a semiquantitative analysis for all samples can be seen in Table 2. H&E stains of control samples confirmed differentiation from primitive, round precursor cells with a high nuclear to cytoplasmatic ratio to spindle cells with a lower nuclear to cytoplasmatic ratio (Figure 3). The samples labeled with 100 $\mu$ g Fe for 4h showed a similar morphology compared to the control samples, while samples labeled with 100 $\mu$ g Fe for 18h or cells that were incubated for 6 or 12 days after 18h labeling showed little differentiation. Cells that were labeled with 50 $\mu$ g Ferucarbotran and Protamine sulfate showed an even lesser degree of differentiation, retaining more the primitive, round-cell phenotype.

Alcian blue staining for glucosaminoglycans was most intense for the control sample (Figure 3). A moderate staining was found for hMSCs that had been incubated with 100 $\mu$ g Fe for 4h and after an additional incubation of 12 days. Weak staining was found after incubation for

18h, after an additional incubation for 6 days and after transfection with protamine (Table 2). In the sample incubated with protamine sulfate, the positive staining by alcian blue is partly obscured by the iron deposition.

## Discussion

The presented data demonstrate a dose-dependent inhibition of chondrogenesis of hMSCs that have been labeled with the SPIO Ferucarbotran. Thus, we confirm results of other groups that described inhibition of chondrogenesis by magnetic labeling with the SPIO Ferumoxides [11]. With our study, we evaluated several variables that may cause the previously described inhibition of chondrogenesis: intracellular iron quantity and presence or absence of extracellular membrane-bound iron. The systematic analysis of spectrometric, histopathologic and ultrastructural data on cellular Ferucarbotran uptake and metabolism led to the development of an improved labeling protocol (100µg Fe/ml for 4h), which does not significantly interfere with chondrogenesis. All labeling protocols led to a strong contrast agent effect on T2 and T2\* images that did not decrease after 14 days of chondrogenic differentiation. The reagents for the proposed labeling procedures are in principle readily clinically applicable in Europe.

Adult hMSCs have been successfully used in vivo in preclinical models for cartilage engineering [27,28]. In a human clinical trial, Centeno et al. have recently reported an increased cartilage volume after transplantation of autologous mesenchymal stem cells [29]. For such applications, noninvasive imaging of the implanted cells would be highly desirable. Experimental studies in animal models showed that direct localization of the engrafted cells allows for early diagnosis of graft failure or cell migration. For example Jing et al. labeled hMSC with Ferumoxides and Protamine sulfate and were able to track such magnetically labeled hMSC by MR imaging over 12 weeks [30]. They discovered by MR imaging that labeled cells did not home to the cartilage defect but migrated to the subchondral bone and the synovium. Thus, they proved the ability to detect graft failure by MR imaging of labeled cells. Interestingly, this finding on MR images was also confirmed for unlabeled cells by histology. Thus, a possibly adverse effect of magnetic labeling can't be the reason for failure to engraft at the site of the cartilage defect. Jing et al suggest a trapping of the injected cells in the exogenous artificial carrier matrix as a reason for the failure to engraft properly. However, intracellular iron content was not measured and can't be eliminated as an additional cause.

Maintained viability of iron oxide-labeled hMSCs is a mandatory prerequisite for any application of stem cells for cell tracking studies. Iron has a well known fundamental role in many cellular metabolic processes, including electron transport, deoxyribonucleotide synthesis, oxygen transport and essential redox reactions involving hemoproteins [31,32]. The incorporation of iron oxides into the normal iron metabolism makes them appealing as contrast agents for cell labeling [33]. But previous studies also showed that iron oxides can impair the viability of stem cells when they are internalized in too high quantities [13,34]. However, if applied in limited concentrations, iron oxides are slowly incorporated into the regular iron metabolism and do not change the physiology of the cells [8,10,11,19,20,34–39]. None of the labeling protocols proposed in this study showed any impairment of cell viability of labeled cells.

Another prerequisite for successful in vivo studies is an unimpaired differentiation capacity of labeled stem cells. Other groups reported normal differentiation of embryonic or neuronal stem cells into neurons after labeling with iron oxides [37,40]. In addition, normal differentiation of hMSCs into chondrocytes [19,20,41] and osteocytes [8,20,41] was noted after labeling with Ferumoxides [8,19,20] or FITC-labeled iron oxide nanoparticles [41]. However another group of investigators reported impaired chondrogenesis of hMSCs after labeling with 50 µg Fe/ml

Ferumoxides-polylysine for a prolonged incubation time of 24 hours [10,11]. This may have been related to the high quantity of internalized contrast agent into the cells, since the same authors found limited chondrogenesis of their cells after incubation with half of the initial contrast agent concentration [11]. Our results – although conducted with a different contrast agent partly confirm these results: we found impaired differentiation of hMSC with an excessive iron load and unimpaired differentiation of hMSCs into chondrocytes, when the cells were labeled with limited doses of iron oxides.

We used the negatively charged iron oxide Ferucarbotran because it is spontaneously endocytosed by hMSC and does not require the use of additional transfection agents [42,43]. However, since Frank et al. reported no effect on the rate of differentiation after the use of the transfection agent Protamine sulfate, we decided to use Ferucarbotran in combination with Protamine sulfate in order to create a comparable experimental setup [19,20]. Similar to studies with Ferumoxides [19], our data shows that the cellular uptake of Ferucarbotran can be significantly increased by the addition of Protamine sulfate.

The analysis of cell morphology of mesenchymal stem cells undergoing chondrogenic differentiation led to the findings that the rate of spindled cells increased during the observed 14 days of chondrogenic differentiation. This is a paradox, because undifferentiated mesenchymal stem cells in vitro are spindle-shaped and chondrocytes in vivo are round. A metaanalysis of histological images in other studies confirmed our findings [11,19,20,44], however, these studies did not analyse cell morphology but staining. Right after trypsinization and at the beginning of chondrogenic differentiation, mesenchymal stem cells are round with a high nuclear to cytoplasmic ratio. This is not the appearance of mature resting chondrocytes, which typically have ample cytoplasm and a small, central nucleus. The difference becomes more evident when looking at undifferentiated cells (Figure 3). During the course of differentiation, we saw an increase in the spindle cell component. We conclude that hMSCs are maturing from a completely round, primitive phenotype, to a more differentiated but still mesenchymal phenotype (with increased cytoplasm but spindled in shape). The cells form a matrix, which is a sign of an intermediate stage of chondrocyte differentiation. However, the cells do not reach the morphology of mature resting chondrocytes with low nuclear to cytoplasmic ratio. It is known, that in the growth plate, the proliferation zone has cells that get compressed and flattened in multicellular clusters [45]. Overall, we conclude that our somewhat paradox finding that is, differentiating chondrocytes appear spindled might be due to the growth in a pellet.

For all labeling protocols using simple incubation, there was an inversely proportional relation between intracellular iron oxide concentration and the rate of chondrogenic differentiation. In fact, the protocol yielding the lowest uptake of iron (100µg Fe/4 hours) showed no significant difference in GAG-synthesis towards the unlabeled control. This supports the theory of a dose-dependent inhibition of chondrogenesis, similar to what Bulte et al. suspected for Ferumoxides-polylysine complexes [11]. However, it has to be considered that iron uptake is inhomogenous and that the amount of internalized iron per cell varies to a certain degree [21,22]. Therefore, even when using the same labeling protocol, the rate of differentiation might vary for each individual cell and results have to be considered valid for a certain population and not for each individual cell.

Our data showed surface-bound iron oxide particles immediately after cell labeling by simple incubation with our standard protocol, whereas there was no surface-bound iron for all other protocol variations. This finding explains why freshly labeled cells with the standard protocol tend to form clumps and are more difficult to resuspend after centrifugation when compared to unlabeled controls. It is known that chondrogenic differentiation depends highly on surface-



linked cellular interactions and needs to be conducted in a 3D culture. It seems likely that surface-bound iron oxide particles could interfere with the essential mechanisms or structures.

Transfection with protamine sulfate yielded the highest iron uptake, about 3 times higher than for our standard protocol. Surprisingly, the total amount of GAG synthesized during differentiation was significantly higher than for the standard protocol (Figure 1). This contradicts a dose-dependency as the only mechanism of the inhibition of chondrogenesis. We offer two possible explanations for this: (1) After labeling with Protamine sulfate, there were no surface bound Ferucarbotran particles that could inhibit surface-linked cell-cell interactions because the transfection agent shuttles the iron oxides into the intracellular compartment more efficiently. (2) Iron oxide filled lysosomes are larger in Protamine sulfate labeled cells than for the other protocols suggesting a different mechanism of uptake or intracellular compartmentalization, which in turn might cause less interaction with differentiation-linked intracellular structures or substrates.

We recognize several limitations to this study. This study was performed on a well-characterized, commercially available cell line of hMSCs, but theoretically, each cell line can behave differently and results might vary for other primary cultures. Although we were able to quantify adverse effects of magnetic labeling on stem cell physiology, the underlying biological mechanisms remain unclear. We confirm similar findings of other groups [10,20,30,46,47] and show that the effects of magnetic labeling will have to be investigated in more detail; this will have to be studied with regards to molecular biology, biochemistry, cell physiology and cell morphology before labeling techniques can be integrated into clinical practice. Furthermore, long-term in vivo studies will have to address the biocompatibility of labeling techniques and the feasibility of this approach for clinical applications.

## SUMMARY

In summary, this study presents practical and efficient labeling techniques for hMSC using the MR contrast agent Ferucarbotran. In an in vitro differentiation model, the presented labeling methods showed different degrees of inhibition of chondrogenic differentiation. By reducing the incubation time and thereby the iron uptake, a higher rate of differentiation was achieved that did not significantly differ from the unlabeled control. These findings emphasize the need for further studies of the biocompatibility of stem cell labeling with iron oxides and other contrast agents before in vivo trials can take place.

## Acknowledgments

This work was in part supported by German Research Foundation (DFG) stipend HE4578/1-2, and by the National Institute of Arthritis and Musculoskeletal and Skin Diseases; Grant Number: NIH R01AR054458

## Literature

1. Pittenger MF, Mackay AM, Beck SC, Jaiswal RK, Douglas R, Mosca JD, Moorman MA, Simonetti DW, Craig S, Marshak DR. Multilineage potential of adult human mesenchymal stem cells. *Science* 1999;284:143–147. [PubMed: 10102814]
2. Deans RJ, Moseley AB. Mesenchymal stem cells: biology and potential clinical uses. *Exp Hematol* 2000;28:875–884. [PubMed: 10989188]
3. Matsubara T, Tsutsumi S, Pan H, Hiraoka H, Oda R, Nishimura M, Kawaguchi H, Nakamura K, Kato Y. A new technique to expand human mesenchymal stem cells using basement membrane extracellular matrix. *Biochem Biophys Res Commun* 2004;313:503–508. [PubMed: 14697217]
4. Curran JM, Chen R, Hunt JA. The guidance of human mesenchymal stem cell differentiation in vitro by controlled modifications to the cell substrate. *Biomaterials* 2006;27:4783–4793. [PubMed: 16735063]

5. Mastrogiacomo M, Muraglia A, Komlev V, Peyrin F, Rustichelli F, Crovace A, Cancedda R. Tissue engineering of bone: search for a better scaffold. *Orthod Craniofac Res* 2005;8:277–284. [PubMed: 16238608]
6. Kuo CK, Ma PX. Ionically crosslinked alginate hydrogels as scaffolds for tissue engineering: part 1. Structure, gelation rate and mechanical properties. *Biomaterials* 2001;22:511–521. [PubMed: 11219714]
7. Petite H, Viateau V, Bensaid W, Meunier A, de Pollak C, Bourguignon M, Oudina K, Sedel L, Guillemain G. Tissue-engineered bone regeneration. *Nat Biotechnol* 2000;18:959–963. [PubMed: 10973216]
8. Bos C, Delmas Y, Desmouliere A, Solanilla A, Hauger O, Grosset C, Dubus I, Ivanovic Z, Rosenbaum J, Charbord P, Combe C, Bulte JW, Moonen CT, Ripoché J, Grenier N. In vivo MR imaging of intravascularly injected magnetically labeled mesenchymal stem cells in rat kidney and liver. *Radiology* 2004;233:781–789. [PubMed: 15486216]
9. Sun JH, Teng GJ, Ju SH, Ma ZL, Mai XL, Ma M. MR tracking of magnetically labeled mesenchymal stem cells in rat kidneys with acute renal failure. *Cell Transplant* 2008;17:279–290. [PubMed: 18522231]
10. Kostura L, Kraitchman DL, Mackay AM, Pittenger MF, Bulte JW. Feridex labeling of mesenchymal stem cells inhibits chondrogenesis but not adipogenesis or osteogenesis. *NMR Biomed* 2004;17:513–517. [PubMed: 15526348]
11. Bulte JW, Kraitchman DL, Mackay AM, Pittenger MF. Chondrogenic differentiation of mesenchymal stem cells is inhibited after magnetic labeling with ferumoxides. *Blood* 2004;104:3410–3412. author reply 3412–3413. [PubMed: 15525839]
12. Boutry S, Brunin S, Mahieu I, Laurent S, Vander Elst L, Muller RN. Magnetic labeling of non-phagocytic adherent cells with iron oxide nanoparticles: a comprehensive study. *Contrast Media Mol Imaging* 2008;3:223–232. [PubMed: 19072771]
13. Metz S, Bonaterra G, Rudelius M, Settles M, Rummeny EJ, Daldrup-Link HE. Capacity of human monocytes to phagocytose approved iron oxide MR contrast agents in vitro. *Eur Radiol* 2004;14:1851–1858. [PubMed: 15249981]
14. Mailander V, Lorenz MR, Holzapfel V, Musyanovych A, Fuchs K, Wiesneth M, Walther P, Landfester K, Schrezenmeier H. Carboxylated superparamagnetic iron oxide particles label cells intracellularly without transfection agents. *Mol Imaging Biol* 2008;10:138–146. [PubMed: 18297365]
15. Henning TD, Wendland MF, Golovko D, Sutton EJ, Sennino B, Malek F, Bauer JS, McDonald DM, Daldrup-Link H. Relaxation effects of ferucarbotran-labeled mesenchymal stem cells at 1.5T and 3T: Discrimination of viable from lysed cells. *Magn Reson Med*. 2009
16. Daldrup-Link HE, Meier R, Rudelius M, Piontek G, Piert M, Metz S, Settles M, Uherek C, Wels W, Schlegel J, Rummeny EJ. In vivo tracking of genetically engineered, anti-HER2/neu directed natural killer cells to HER2/neu positive mammary tumors with magnetic resonance imaging. *Eur Radiol* 2005;15:4–13. [PubMed: 15616814]
17. Reimer P, Balzer T. Ferucarbotran (Resovist): a new clinically approved RES-specific contrast agent for contrast-enhanced MRI of the liver: properties, clinical development, and applications. *Eur Radiol* 2003;13:1266–1276. [PubMed: 12764641]
18. Wang YX, Hussain SM, Krestin GP. Superparamagnetic iron oxide contrast agents: physicochemical characteristics and applications in MR imaging. *Eur Radiol* 2001;11:2319–2331. [PubMed: 11702180]
19. Arbab AS, Yocum GT, Kalish H, Jordan EK, Anderson SA, Khakoo AY, Read EJ, Frank JA. Efficient magnetic cell labeling with protamine sulfate complexed to ferumoxides for cellular MRI. *Blood* 2004;104:1217–1223. [PubMed: 15100158]
20. Arbab AS, Yocum GT, Rad AM, Khakoo AY, Fellowes V, Read EJ, Frank JA. Labeling of cells with ferumoxides-protamine sulfate complexes does not inhibit function or differentiation capacity of hematopoietic or mesenchymal stem cells. *NMR Biomed* 2005;18:553–559. [PubMed: 16229060]
21. Omidkhoda A, Mozdarani H, Movasaghpoor A, Fatholah AA. Study of apoptosis in labeled mesenchymal stem cells with superparamagnetic iron oxide using neutral comet assay. *Toxicol In Vitro* 2007;21:1191–1196. [PubMed: 17493781]

22. Song M, Moon WK, Kim Y, Lim D, Song IC, Yoon BW. Labeling efficacy of superparamagnetic iron oxide nanoparticles to human neural stem cells: comparison of ferumoxides, monocrystalline iron oxide, cross-linked iron oxide (CLIO)-NH<sub>2</sub> and tat-CLIO. *Korean J Radiol* 2007;8:365–371. [PubMed: 17923778]
23. Hashimoto J, Kariya Y, Miyazaki K. Regulation of proliferation and chondrogenic differentiation of human mesenchymal stem cells by laminin-5 (laminin-332). *Stem Cells* 2006;24:2346–2354. [PubMed: 17071854]
24. Ponticello MS, Schinagl RM, Kadiyala S, Barry FP. Gelatin-based resorbable sponge as a carrier matrix for human mesenchymal stem cells in cartilage regeneration therapy. *J Biomed Mater Res* 2000;52:246–255. [PubMed: 10951362]
25. Farndale RW, Sayers CA, Barrett AJ. A direct spectrophotometric microassay for sulfated glycosaminoglycans in cartilage cultures. *Connect Tissue Res* 1982;9:247–248. [PubMed: 6215207]
26. Wolff SD, Balaban RS. Assessing contrast on MR images. *Radiology* 1997;202:25–29. [PubMed: 8988186]
27. Koga H, Muneta T, Nagase T, Nimura A, Ju YJ, Mochizuki T, Sekiya I. Comparison of mesenchymal tissues-derived stem cells for in vivo chondrogenesis: suitable conditions for cell therapy of cartilage defects in rabbit. *Cell Tissue Res* 2008;333:207–215. [PubMed: 18560897]
28. Murphy JM, Fink DJ, Hunziker EB, Barry FP. Stem cell therapy in a caprine model of osteoarthritis. *Arthritis Rheum* 2003;48:3464–3474. [PubMed: 14673997]
29. Centeno CJ, Busse D, Kisiday J, Keohan C, Freeman M, Karli D. Increased knee cartilage volume in degenerative joint disease using percutaneously implanted, autologous mesenchymal stem cells. *Pain Physician* 2008;11:343–353. [PubMed: 18523506]
30. Jing XH, Yang L, Duan XJ, Xie B, Chen W, Li Z, Tan HB. In vivo MR imaging tracking of magnetic iron oxide nanoparticle labeled, engineered, autologous bone marrow mesenchymal stem cells following intra-articular injection. *Joint Bone Spine* 2008;75:432–438. [PubMed: 18448377]
31. Shaw GC, Cope JJ, Li L, Corson K, Hersey C, Ackermann GE, Gwynn B, Lambert AJ, Wingert RA, Traver D, Trede NS, Barut BA, Zhou Y, Minet E, Donovan A, Brownlie A, Balzan R, Weiss MJ, Peters LL, Kaplan J, Zon LI, Paw BH. Mitoferrin is essential for erythroid iron assimilation. *Nature* 2006;440:96–100. [PubMed: 16511496]
32. Ivanovic Z. Hemopoietic stem cell proliferation in Belgrade rats: to complete the parable. *Hematol Cell Ther* 1997;39:307–316. [PubMed: 9497890]
33. Jung CW. Surface properties of superparamagnetic iron oxide MR contrast agents: ferumoxides, ferumoxtran, ferumoxsil. *Magn Reson Imaging* 1995;13:675–691. [PubMed: 8569442]
34. Daldrup-Link HE, Rudelius M, Oostendorp RA, Settles M, Piontek G, Metz S, Rosenbrock H, Keller U, Heinzmann U, Rummeny EJ, Schlegel J, Link TM. Targeting of hematopoietic progenitor cells with MR contrast agents. *Radiology* 2003;228:760–767. [PubMed: 12881578]
35. Terrovitis JV, Bulte JW, Sarvananthan S, Crowe LA, Sarathchandra P, Batten P, Sachlos E, Chester AH, Czernuszka JT, Firmin DN, Taylor PM, Yacoub MH. Magnetic resonance imaging of ferumoxide-labeled mesenchymal stem cells seeded on collagen scaffolds-relevance to tissue engineering. *Tissue Eng* 2006;12:2765–2775. [PubMed: 17518646]
36. Rogers WJ, Meyer CH, Kramer CM. Technology insight: in vivo cell tracking by use of MRI. *Nat Clin Pract Cardiovasc Med* 2006;3:554–562. [PubMed: 16990841]
37. Watson DJ, Walton RM, Magnitsky SG, Bulte JW, Poptani H, Wolfe JH. Structure-specific patterns of neural stem cell engraftment after transplantation in the adult mouse brain. *Hum Gene Ther* 2006;17:693–704. [PubMed: 16839269]
38. Hinds KA, Hill JM, Shapiro EM, Laukkanen MO, Silva AC, Combs CA, Varney TR, Balaban RS, Koretsky AP, Dunbar CE. Highly efficient endosomal labeling of progenitor and stem cells with large magnetic particles allows magnetic resonance imaging of single cells. *Blood* 2003;102:867–872. [PubMed: 12676779]
39. Rudelius M, Daldrup-Link HE, Heinzmann U, Piontek G, Settles M, Link TM, Schlegel J. Highly efficient paramagnetic labelling of embryonic and neuronal stem cells. *Eur J Nucl Med Mol Imaging* 2003;30:1038–1044. [PubMed: 12567250]
40. Hoehn M, Kustermann E, Blunk J, Wiedermann D, Trapp T, Wecker S, Focking M, Arnold H, Hescheler J, Fleischmann BK, Schwandt W, Buhle C. Monitoring of implanted stem cell migration

- in vivo: a highly resolved in vivo magnetic resonance imaging investigation of experimental stroke in rat. *Proc Natl Acad Sci U S A* 2002;99:16267–16272. [PubMed: 12444255]
41. Lu CW, Hung Y, Hsiao JK, Yao M, Chung TH, Lin YS, Wu SH, Hsu SC, Liu HM, Mou CY, Yang CS, Huang DM, Chen YC. Bifunctional magnetic silica nanoparticles for highly efficient human stem cell labeling. *Nano Lett* 2007;7:149–154. [PubMed: 17212455]
  42. Henning, TD.; Bauer, JS.; Frenzel, T.; Surrón, EJ.; Fu, Y.; Daldrup-Link, HE. Long term MR signal characteristics of Ferucarbotran-labeled mesenchymal stem cells: Discrimination of intra- and extracellular iron oxides before and after cell lysis. 14th Scientific Meeting of the International Society of Magnetic Resonance in Medicine; Seattle. 2006.
  43. Hsiao JKTM, Chu HH, Chen ST, Li H, Lai DM, Hsieh ST, Wang JL, Liu HM. Magnetic nanoparticle labeling of mesenchymal stem cells without transfection agent: cellular behavior and capability of detection with clinical 1.5 T magnetic resonance at the single cell level. *Magn Reson Med* 2007;58:717–724. [PubMed: 17899592]
  44. Ebisawa K, Hata K, Okada K, Kimata K, Ueda M, Torii S, Watanabe H. Ultrasound enhances transforming growth factor beta-mediated chondrocyte differentiation of human mesenchymal stem cells. *Tissue Eng* 2004;10:921–929. [PubMed: 15265310]
  45. Mackie EJ, Ahmed YA, Tatarczuch L, Chen KS, Mirams M. Endochondral ossification: how cartilage is converted into bone in the developing skeleton. *Int J Biochem Cell Biol* 2008;40:46–62. [PubMed: 17659995]
  46. Tallheden T, Nannmark U, Lorentzon M, Rakotonirainy O, Soussi B, Waagstein F, Jeppsson A, Sjogren-Jansson E, Lindahl A, Omerovic E. In vivo MR imaging of magnetically labeled human embryonic stem cells. *Life Sci* 2006;79:999–1006. [PubMed: 16828117]
  47. Schafer R, Kehlbach R, Wiskirchen J, Bantleon R, Pintaske J, Brehm BR, Gerber A, Wolburg H, Claussen CD, Northoff H. Transferrin Receptor Upregulation: In Vitro Labeling of Rat Mesenchymal Stem Cells with Superparamagnetic Iron Oxide. *Radiology* 2007;244:514–523. [PubMed: 17562811]

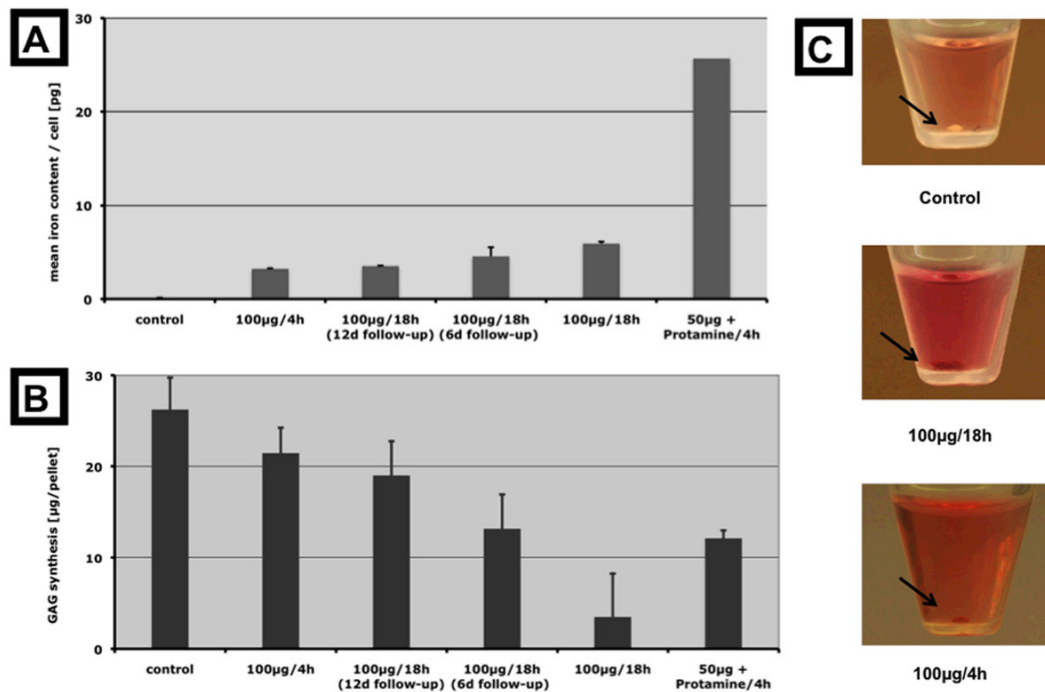


**Figure 1.**

The different samples are arranged along the x-axis according to their iron content. Graph A shows the mean uptake of iron per cell immediately after labeling of undifferentiated hMSC (n = 3). Graph B displays the average amount of glucosaminoglycans synthesized after 14 days of chondrogenic differentiation by the different pellets (n = 3). Except for the cells incubated with protamine sulfate, the relation between chondrogenic differentiation and cellular iron uptake is inversely proportional. Photographs (C) show chondrogenic pellets (black arrows). Note the brown coloring of the labeled pellets due to the iron oxides.



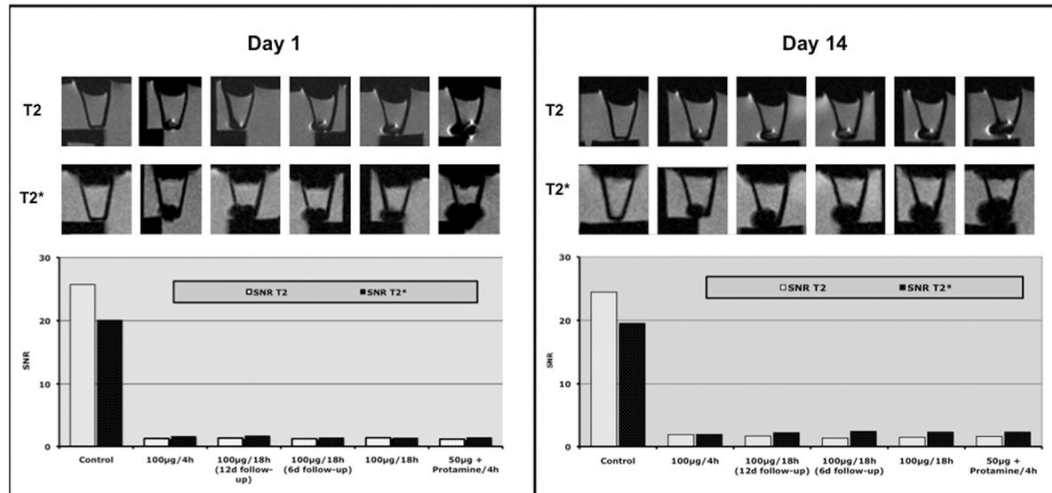


**Figure 2.** MR imaging at 3T of chondrogenic pellets at 3T at day 1 and day 14 of differentiation (n = 1). The MR images demonstrate the contrast agent effect of all labeled chondrogenic pellets as acquired with axial T2 SE- (TR 2000/TE 15) and T2\*GE-sequences (TR 500/TE 14). The bar graph shows the signal-to-noise ratio for all samples as acquired with these sequences. Of note: The black bars under the centrifuge tubes correspond to the rack used for positioning the tubes in the water bath.

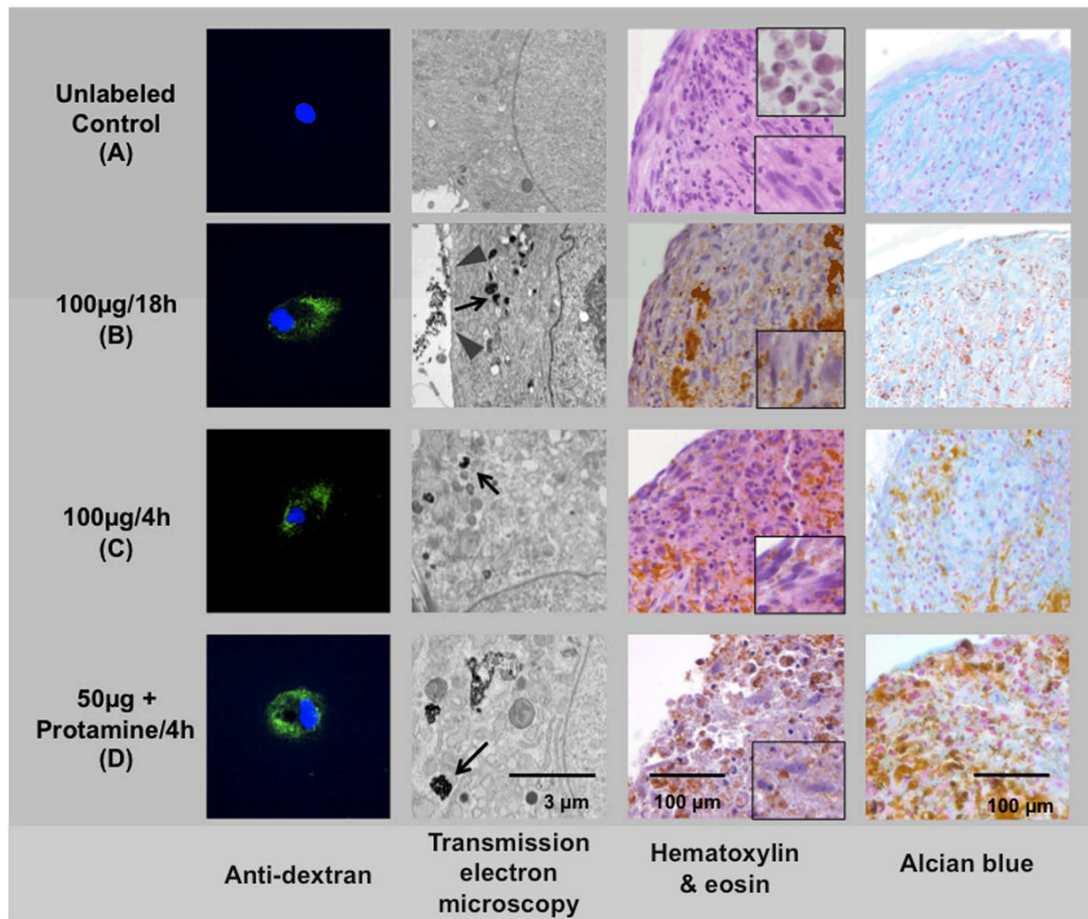


**Figure 3.**

Comparison of different labeling protocols versus unlabeled control: Anti-dextran staining of undifferentiated hMSC (green) demonstrates intracellular localization of contrast agent within the labeled cells (first column). Electron microscopy images of all undifferentiated labeled hMSC samples depict iron oxide particles within secondary lysosomes (second column, black arrows in B, C, D). Note the membrane-adsorbed iron oxide particles after labeling with 100 µg Fe for 18 h (gray arrowhead in B). H&E and alcian blue staining (third and fourth column) of differentiated cell pellets show different grades of chondrogenesis. Note the differentiated spindled cells in the magnified window (lower right corner, third column, A-C) versus the undifferentiated round cells (upper right corner, third column, A). The brown deposits on H&E and Alcian blue stains indicate iron oxide particles. Note: The high density of these contrast agent particles compared to the electron microscopy images are due to the thin slice thickness (80 nm vs 5 µm) and the high magnification of electron microscopy images.

**Table 1****Cell labeling data**

Mean iron content and cell viability were assessed for undifferentiated hMSC immediately after labeling and washing. An asterisk indicates a significant difference from the unlabeled control. Viability was not significantly affected by any of the labeling protocols.

Labeling protocol	Iron content [pg/cell]	Viability
Control	0.06 ( $\pm$ 0.06)	97.33% ( $\pm$ 1.53%)
100 $\mu$ g Fe, 4h	3.21 ( $\pm$ 0.21) *	96.33% ( $\pm$ 2.52%)
100 $\mu$ g Fe/18h (12d follow-up)	3.50 ( $\pm$ 0.14) *	96.33% ( $\pm$ 2.08%)
100 $\mu$ g Fe/18h (6d follow-up)	4.55 ( $\pm$ 0.87) *	96.67% ( $\pm$ 1.53%)
100 $\mu$ g Fe/18h	5.90 ( $\pm$ 0.76) *	96.67% ( $\pm$ 2.98%)
50 $\mu$ g + Protamine/4h	25.65 ( $\pm$ 0.96) *	95.00% ( $\pm$ 2.65%)

\* = significantly different from control (p < 0.05)

**Table 2****Histology quantitation**

Semiquantitative Analysis of histopathology of chondrogenic pellets. Differentiation into spindle-like cells was quantified on a scale from 0–3 and intensity of alcian blue staining for deposition of Glucosaminoglycans was quantified by “–” and “+” indicating negative or positive staining.

Labeling protocol	Hematoxilin & Eosin (H&E)	Alcian blue
Control	2	+++
100µg Fe, 4h	2	++
100µg Fe/18h (12d follow-up)	1	++
100µg Fe/18h (6d follow-up)	1	+
100µg Fe/18h	1	+
50ug + Protamine/4h	1	+

scores: 0 = no spindled cells

1 = 1 – 33% spindled cells

2 = 33 – 66% spindled cells

3 = 66 – 100 % spindled cells

+ = weak staining

++ = moderate staining

+++ = most intense staining